PCCP

PAPER

View Article Online
View Journal | View Issue

Cite this: *Phys. Chem. Chem. Phys.*, 2018, **20**, 26853

Ostwald's rule of stages and metastable transitions in the hydrogen–water system at high pressure†

M.-E. Donnelly,[a] P. Teeratchanan,[a] C. L. Bull,[b] A. Hermann[a] and J. S. Loveday *[a]

Received 14th July 2018,
Accepted 10th October 2018

DOI: 10.1039/c8cp04464c

rsc.li/pccp

Although the hydrogenous analogue of the D_2–D_2O system has been well explored in the regimes above 1 GPa, and below 0.2 GPa, there have been very few studies in the region between these pressures. The recent discovery in the range 0.5–0.7 GPa of a new phase, C_0, that possesses a new clathrate structure with a new H_2O network, along with the proposal of another structure stable at similar conditions, has prompted further studies of the hydrogen water system in this intermediate pressure region. Here, we report the results of neutron-diffraction experiments that observed transitions from metastable to stable structures in the D_2–D_2O system around 0.2–0.3 GPa between 130 K and 280 K. These metastable structures were observed in the stability region of the sII hydrogen hydrate clathrate and computational studies of their relative enthalpies suggest that transition sequence observed is in line with Ostwald's 'Rule of Stages'.

1 Introduction

It is well known that water combines with many simple gases to form crystalline compounds known as gas hydrates. These 'host–guest' compounds have H_2O molecules arranged in hydrogen-bonded cage or channel structures around the 'guest' gas molecules or atoms, and the host and guest interact through van der Waals forces. Gas hydrates are generally found to be stable at high pressures and/or low temperatures and their stability range is strongly dependent on the gas species. Gas hydrates are of interest because they provide access to hydrogen bond topologies not found in pure ice structures and may have applications as gas storage/separation materials.[1–4] For such applications, a crucial parameter is the gas : water ratio which should be as high as possible. Pressure is a useful tool in the search for gas-richer phases because the proportion of gas in gas hydrate structures tends to increase with pressure.[1,5]

The hydrogen–water system is a good example of such a system. There is a clear need for hydrogen storage materials, and pressure improves the hydration ratio.[3,5–7] To date there have been four phases reported experimentally (Fig. 1).

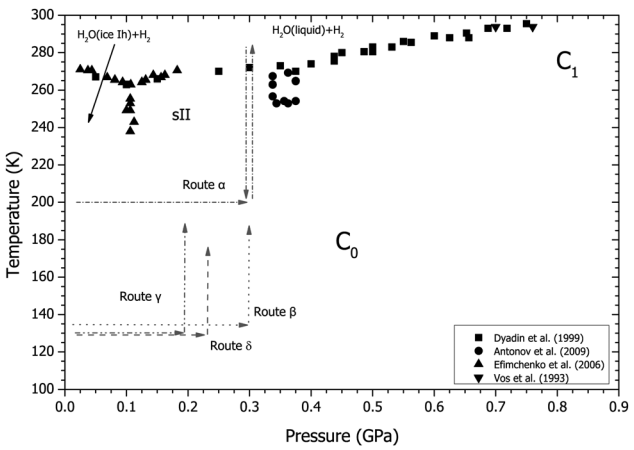

Fig. 1 Phase diagram of the H_2–H_2O system showing previous experimental determinations of the phase boundaries shown as squares,[19] circles,[20] up triangles[21] and down triangles.[5] The four routes taken through P–T space (α, β, γ and δ) are marked on the diagram with dashed and/or dotted arrows.

The lowest pressure phase, sII, adopts the type II cubic clathrate structure with an H_2O : H_2 ratio of almost 3 : 1.[8,9] As pressure is increased, at ~0.5 GPa the so called C_0 hydrate becomes the most stable phase with a H_2O : H_2 ratio of 2 : 1 and the spiral cage-like structure, S_χ.[10–14] This structure is surprisingly also found in the carbon dioxide:water system.[14] At ~1 GPa C_1 hydrate becomes the most stable phase with a crystal structure based on ice II with H_2 molecules occupying the hexagonal

[a] SUPA, School of Physics and Astronomy and Centre for Science at Extreme Conditions, The University of Edinburgh, Edinburgh, EH9 3JZ, UK. E-mail: j.loveday@ed.ac.uk
[b] ISIS Neutron Facility, STFC Rutherford Appleton Lab, Chilton, Oxon, OX11 0QX, UK

† Electronic supplementary information (ESI) available. See DOI: 10.1039/c8cp04464c

channels of this structure with an assumed $H_2O:H_2$ ratio of 6 : 1.[5] Above 2 GPa, C_2 hydrate is the most stable phase with a cubic crystal-structure based on ice Ic with a $H_2O:H_2$ ratio of 1 : 1.[5] Thus the H_2–H_2O system shows a propensity to form hydrates whose structures are based on those of ice phases. However, there have been no experimentally reported filled ice Ih structures within this system. The filled ice Ih structure has been previously observed in the methane–, argon–, krypton– and nitrogen–water systems.[1] Recently, a filled ice Ih type structure was proposed to be stable at the same the conditions as the C_0 phase in the H_2–H_2O system by Qian *et al.* using an evolutionary structure search.[15] Here we report results from a neutron-diffraction experiments on the D_2–D_2O system at low pressures – in the stability region of the sII hydrate.[16] In these we observed the inclusion of deuterium into an ice Isd structure (a stacking disordered structure of ices Ih and Ic),[17,18] and the appearance of the C_0 structure outside its stability range.

2 Experimental details

A hydrogen-compatible aluminium gas cell rated to 0.3 GPa was loaded with powdered deuterated ice at 77 K. The cell was sealed, compressed to ~100 bar with deuterium gas, and transferred to an "Orange" (Institut Laue Langevin pattern) cryostat. The pressure was varied using a "capstan" pump. Several routes were taken to explore what effect changing pressure and temperature had on the formation of the structures observed and these are indicated in Fig. 1. All routes started at ~100 bar in a D_2 atmosphere at 200 K with the sample in the form of ice Ih. In route α the sample was compressed from these initial conditions to 0.3 GPa at 200 K. It was then warmed above the melt curve at 280 K before cooling to 200 K. In route β the sample was initially cooled to 135 K at ~100 bar then compressed to 0.3 GPa with D_2 and warmed to 180 K. Routes γ and δ follow the same initial route as β however, instead of compression to 0.3 GPa the sample was compressed to 0.2 and 0.23 GPa, respectively. Each sample compression took approximately 10 minutes. Data were collected with *in situ* neutron diffraction on the PEARL[22] instrument at the ISIS neutron source at the Rutherford Appleton Laboratory before normalisation correction for attenuation by the gas cell using the Mantid suite.[23] Analysis of the diffraction patterns was carried out by either Rietveld or Le Bail profile refinement using the GSAS crystallographic software suite.[24]

3 Computational details

Electronic structure calculations within the framework of density functional theory (DFT) were performed using the projector-augmented wave method in conjunction with a plane-wave basis set as implemented in the VASP code.[25,26] A plane-wave cutoff of E_c = 800 eV and reciprocal-space sampling-density of 20 *k*-points per $Å^{-1}$ were used. All structures were optimised until remaining forces were below 1 meV $Å^{-1}$. Stability of hydrates was evaluated against pure ices (including XI, II, XIII, XIV, XV, and VIII) and hydrogen phase-I (modelled in a eight molecule $P6_3/m$ unit cell). The non-local vdW-DF approach, which accounts for dispersion interactions, was used to approximate electron exchange–correlation effects, using the optB88 exchange functional.[27–30]

4 Results

4.1 Pressure and temperature route α

Immediately after compression to 0.3 GPa at 200 K (see Fig. 1 and 2), the ice Ih converted into the C_0 structure (see ESI† for full structural information). The diffraction data collected at this point and in the subsequent warm-up/cool-down cycle are shown in Fig. 2. The sample was warmed slowly in steps of 5 K and at 260 K new peaks started to appear (Fig. 2). These peaks were identified as those of the sII phase of hydrogen hydrate. As temperature was increased further, the peaks from sII grew in intensity whilst the peaks arising from the C_0 structure decreased. The conversion of the sample from the C_0 structure to the sII structure was also accompanied by a large increase in the gas pressure, indicating an increase in overall sample volume on transformation to sII – *i.e.* that the C_0 structure was either denser, and/or richer in D_2 than sII. It was not possible to quantify the absolute change in pressure for safety reasons as the gas cell was already operating at the maximum safe pressure of 0.3 GPa and any evolved gas had to be immediately vented. The sample was heated further and at 280 K sII decomposed into gas and a liquid (it is assumed that this liquid contains dissolved deuterium). This discrepancy in the decomposition temperature (~10 K above where the sII phase in the H_2–H_2O system decomposes) is attributed to a slight hysteresis effect and not an isotopic effect as the sample started to reform the sII structure between 280 K and 270 K upon cooling. Further cooling resulted in the sample forming a mixture of sII and pure ice II at 250 K (see diffraction patterns in Fig. 2). The lattice parameters for both the sII and pure ice II structures at these conditions (a = 17.107(2) Å and a = 7.7846(3) Å/α = 113.113(1)°, respectively) are in good agreement with those of the literature values.[1,8,31] The sample was further cooled to 200 K and was left at the same conditions

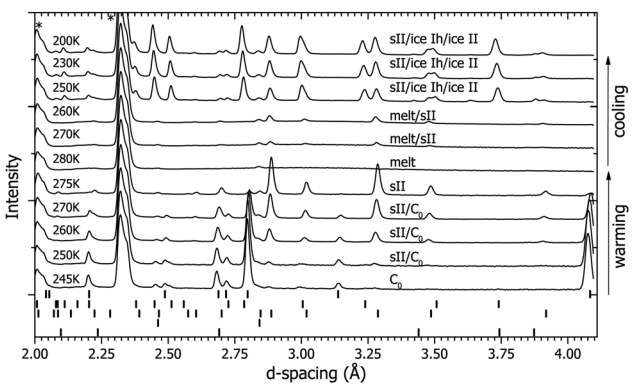

Fig. 2 Route α: diffraction patterns obtained at 0.3 GPa on warming from 245 K to 280 K, and on cooling from 280 K to 200 K. Asterisks indicate peaks from the aluminium of the gas cell. Tick marks indicate reflections, from top to bottom, of C_0, ice II, sII clathrate, lead (gas-cell seal) and ice Ih.

C_0 had previously formed at (0.3 GPa and 200 K) before the warm up. However, after 10 hours there were no reflections from C_0 observed in the diffraction pattern. The non-formation of the C_0 structure at the same conditions as the previous observation suggest that the sII phase is the most stable configuration at this pressure and the previous formation of C_0 at 0.3 GPa and 200 K is attributed to trapping of the metastable C_0 structure. It is of course possible that non-formation of C_0 on cooling at 0.3 GPa is caused by slow kinetics but we reject this possibility on the grounds that C_0 was observed to form rapidly from ice Ih at a lower temperature upon the initial pressurisation (see above).

4.2 Route β

Route β (see Fig. 1 and 3) was followed to investigate the impact of temperature on the formation of C_0. After the formation of ice Ih at 200 K the sample was cooled to 135 K at ~100 bar then compressed to 0.3 GPa with D_2. At this point the diffraction pattern is still described by ice Ih (see Fig. 3) despite the ice II (in pure ice) or sII (in H_2–H_2O) phases being the most stable under these conditions. The sample was heated and at 150 K it converted into a new structure, which we call C_{-1}, and is either a filled ice Isd structure or filled ice Ih structure depending on the 'starter' ice (for more details see ESI†).[17,18] The temperature was increased further, and at 180 K the sample converted into the C_0 structure.

4.3 Route γ

After compression to 0.2 GPa at 130 K (see Fig. 1 and 4) the diffraction pattern showed the sample to have the ice Ih structure (see Fig. 4), which is expected as these conditions are right on the boundary between ice Ih/Ic, II and IX/III.[32] As the sample was heated, splitting of some of the ice Ih reflections was observed, for example those at ~3.4 Å and ~3.85 Å in Fig. 4 at 170–180 K. This splitting is attributed to the appearance of a new structure. At 185 K the sample converted into a mixture of sII and C_0, and at 190 K all the diffraction peaks can be fitted with the sII clathrate structure.

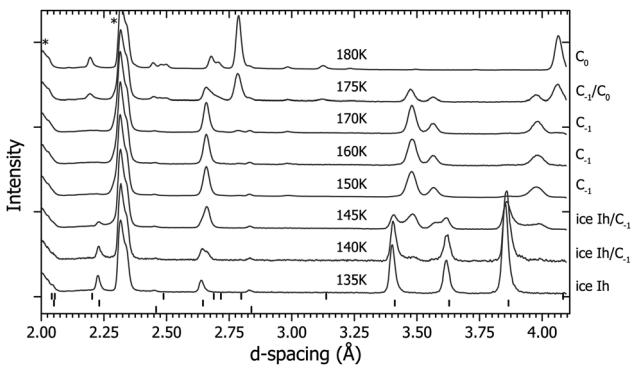

Fig. 3 Route β: diffraction patterns obtained at 0.3 GPa on warming from 135 K to 180 K. Asterisks mark aluminium reflections from the gas cell. Tick marks indicate peaks that can be indexed as reflections from C_0 (top), ice Ih (middle), and lead (gas-cell seal, bottom). The remaining unmarked peaks are attributed to the new C_{-1} structure.

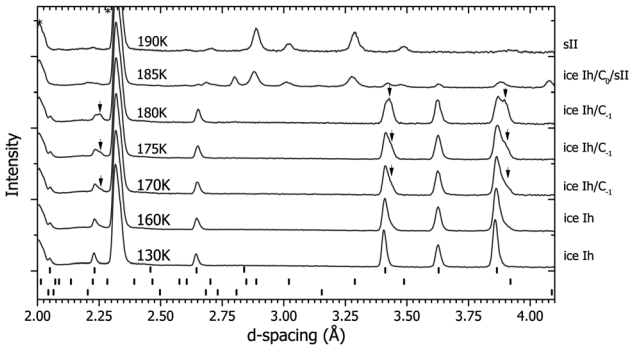

Fig. 4 Route γ: diffraction patterns on warming between 130–190 K at 0.2 GPa. Asterisks mark reflections from the aluminium gasket. Tick marks indicate peaks that can be indexed as reflections from ice Ih (top), sII (middle) and C_0 (bottom). Arrows indicate the peaks and shoulders that are attributed to the formation of C_{-1}.

Data collected on this route were used to determine the crystal structure of C_{-1}. The structure is described by the space group $P6_3/mmc$ with lattice parameters a = 4.5160(7) Å and c = 7.2691(18) Å at 180 K/0.2 GPa. The D_2O continues to adopt an ice Ih based network and the guest D_2 occupy the channels within this structure (see Table 1 for crystallographic information and the ESI† further details). Under these low pressures the guest deuterium molecules are believed to be highly mobile as they are in sII and C_0, and so the fractional occupancy, atomic position and thermal parameter given in Table 1 are approximations.[9,14] The C_{-1} structure was also found to be highly dependent on the 'starter ice'. For example, if a sample of C_{-1} was synthesised from a powder of ice Ih then the resultant C_{-1} crystal structure could be described by the filled ice Ih structure given in Table 1. However, if the 'starter ice' was ice Isd – a type of stacking-faulted ice (see Section 4.4) – then the filled ice Ih structure was unable to describe the observed diffraction pattern from the 'C_{-1}' structure formed. Instead it is thought that the guest gas molecules 'fill' the structure with little disturbance to the host D_2O framework of the starter material. Evidence from a recovered sample of C_{-1} formed from ice Isd showing this effect can be found in the ESI.† Unfortunately, a full Rietveld refinement of the filled ice Isd structure was unstable due to the difficulty in separating the cubic and hexagonal contributions to the diffraction pattern due to overlapping reflections, and determination of the deuterium uptake of the cubic/hexagonal fractions and boundaries in ice Isd (see ESI†).

4.4 Route δ

Upon decompression from the final structure observed on route γ, the sII clathrate converted into ice Isd[17,33] – a stacking-faulted structure which is intermediate between ice Ih and ice Ic whose diffraction pattern in this case can still be indexed as ice Ih in the diffraction patterns (Fig. 5). Although the structure can still be indexed as ice Ih, the presence of ice Isd is characterized by the region of raised intensity between 3.43 and 3.86 Å.[17] Ice Isd (formerly often referred to as ice Ic) is observed as the product when high-pressure ice phases are recovered to ambient

Table 1 Lattice parameters/volume, thermal parameter of the D_2O host and D_2 guest, atomic coordinates and bond lengths/bond angles of the D_2O network of the C_{-1} structure at 0.2 GPa and 180 K. Atom subscripts are used as descriptors and do not refer to molecules in the case of D_2. As the guest deuterium molecules were modelled in the refinements by one atom with large variable isotropic thermal parameters and site occupancy, the D_{guest} described here shows the occupancy of that site and so the molecular deuterium occupancy of the guest site is then half of that shown

C_{-1} structure at P = 0.2 GPa, T = 180 K
Quality of fit: R_{wp} = 6.10%
Space group: $P6_3/mmc$
a = 4.5160(7) Å, c = 7.2691(18) Å, V = 128.39(3) Å^3
U_{iso}(host) = 2.1(1) × 10^{-2} Å^2
U_{iso}(guest) = 10.0(1) × 10^{-2} Å^2

Atom	Site	x	y	z	F
O_1	4f	0.3333	0.6667	0.0556(2)	1.0
D_1	4f	0.3333	0.6667	0.2007(3)	0.5
D_2	12k	0.4571(2)	0.9141(2)	0.0229(3)	0.5
D_{guest}	2b	0	0	0.25	0.55(3)

Bond	Length (Å)	Bond	Angle (degrees)
O_1–D_1	1.0547(3)	D_2–O_1–D_2	114.50(2)
O_1–D_2	0.9964(1)	D_1–O_1–D_2	103.79(1)
$O_1\cdots O_1$	2.7299(3)		
$O_1\cdots O_1$	2.8256(7)		

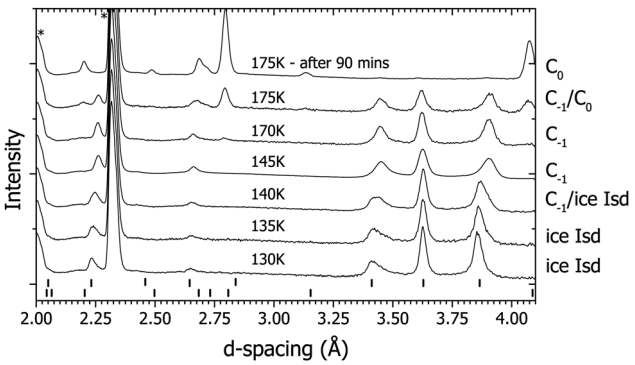

Fig. 5 Route δ: diffraction patterns from warming between 130–175 K at 0.23 GPa. Asterisks mark reflections from the aluminium gas cell. Tick marks indicate peaks that can be indexed as reflections from ice Isd (top) and C_0 (bottom).

pressure and warmed.[17,33] An attempt was made to convert the ice Isd into ice Ih by heating to 230 K, but the ice Isd persisted to this temperature. Another way to turn the ice Isd into ice Ih would have been to melt then refreeze the water, however this would have resulted in a poor powder so it was deemed better to continue with ice Isd than to risk losing a well randomised powder. The sample was cooled to 130 K and compressed to 0.23 GPa with D_2 (see Fig. 1 and 5) and then heated. At 140 K a similar behaviour was observed with the broadening of peaks attributed to ice Ih at ∼3.4 Å and ∼3.85 Å as was observed in route γ at 0.2 GPa (Fig. 4). As temperature was increased to 145 K, the broadening that was observed at 140 K turned out to be the growth of the new structure. At 145 K the contraction of the peak at ∼3.65 Å was observed (Fig. 5) which suggests that this new structure is actually the lower pressure form of the C_{-1} structure observed at 0.3 GPa. The temperature was increased further and at 175 K the C_0 phase started to grow. At this point the gas pressure started to drop rapidly indicating either an extremely dense structure had formed or the sample was absorbing D_2. After ∼90 minutes the gas pressure remained constant indicating the sample had absorbed all the gas it was capable of absorbing. The diffraction pattern showed that it had fully converted to the C_0 phase (top diffraction pattern in Fig. 5).

Though the phase boundaries of the H_2–H_2O system are relatively well known they are not for the D_2–D_2O system.[5,10,11,19] At 0.3 GPa and 200 K the sample is quite near the phase boundary between sII and the suspected region where C_0 is stable.[10,11] There is the possibility that the observation of the C_0 structure was just due to the phase boundaries being different in the deuterated system. This possibility was ruled out by returning to same conditions *via* a different route (cooling from the melt in route α) and C_0 was not observed. Thus the C_0 structure is thought to be metastable at 0.3 GPa in the temperature region studied. A previous neutron diffraction study was done by Lokshin *et al.* at 0.21 GPa where they cooled from above 200 K to 40 K in which they report no observation of C_0 or any other structure such as an ice Isd based structure like C_{-1}.[9] This suggests that at 0.2 GPa the formation of both the C_0 and C_{-1} structures were also metastable with respect to sII.

4.5 DFT calculations

Total energy DFT calculations were performed to determine if the structures observed are metastable at 0.2–0.3 GPa. For the C_0 hydrate, we assumed a hydrogen-ordered water network and full occupancy of the guest sites, leading to a 2:1 host–guest ratio; this is in calculations the most stable C_0 hydrate.[14] The C_{-1} hydrate was modelled with fully occupied H-sites at the centers of the cages in the antiferroelectric ice-XI water network (space group $Pna2_1$), to give a 2:1 hydrate. The calculated formation enthalpies ΔH_f of both C_0 and C_{-1}, relative to decomposition into the respective most stable ice phase and solid hydrogen are shown in Fig. 6. There, we also show the

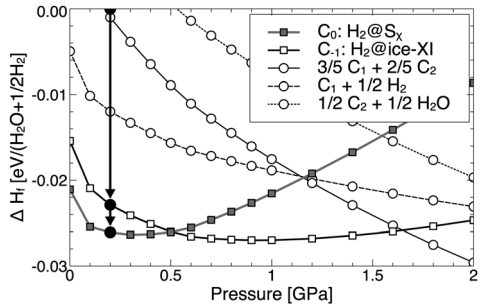

Fig. 6 Enthalpies of formation of C_0 and C_{-1} (grey and white squares), and of other hydrates and constituents in a 2 : 1 water : hydrogen ratio (circles), all shown relative to decomposition into the constituents ice and hydrogen. Arrows indicate successive stabilisation at 2 kbar along the sequence ice → C_{-1} → C_0.

reaction enthalpies of possible competing formation of C_1 and C_2 hydrates, considering excess hydrogen or ice as appropriate. The C_1 and C_2 hydrates were modelled in $R\bar{3}$ and $I4_1md$ structures that correspond to fully filled ice-II and ice-Ic water networks, and thus represent 6 : 1 and 1 : 1 hydrates, respectively. In the pressure region of 0.2–0.3 GPa both C_{-1} and C_0 hydrate are stable against decomposition into ice and H_2, and against the formation of the higher hydrates (we did not consider the sII structure here). The energetic order of C_{-1} and C_0 reverses at 0.5 GPa, in line with literature findings.[15] Around 1.7 GPa, the calculations predict that C_{-1} would decompose into a linear combination of C_1 and C_2 hydrates. The main results of the calculations – that C_0 is more stable than C_{-1} at low pressures and C_{-1} eventually decomposes into higher hydrates – are independent of the choice of exchange–correlation functional, though values for transition pressures do vary.[34]

5 Discussion & conclusions

Our results suggest the following view of the free energy landscape. When ice Ih was compressed above 0.2 GPa at 135 K it was no longer the lowest in free energy and thus no longer the most stable state. As the sample was warmed it transformed into a metastable state (C_{-1}) that was lower in free energy than ice Ih at 0.3 GPa but higher than that of C_0. As the sample was heated further it acquired enough energy to overcome the energy barrier to fall into the next local minimum in the free energy landscape, C_0, and upon further heating the sample overcame the energy barrier to form sII clathrate which appears to be the global minimum of the free energy landscape at 0.3 GPa.

If the results of the three routes explored are combined together they give a general transition sequence of ice Ih → C_{-1} → C_0 → sII at both 0.2 and 0.3 GPa on warming. At these pressures ice Ih based structures are less stable than C_0 for hydrogen hydrate.[15,35] This means the sample goes through a series of transitions that occur in increasing stability. This cascading through metastable states from an unstable state (ice Ih in this case) to most stable (sII clathrate) is known as Ostwald's Rule of Stages (also known as Law of Steps).[36,37] Ostwald's Rule of Stages has long been reported to occur in colloidal crystals, proteins and only very recently in smaller molecular or atomic systems when crystallising from the melt or amorphous material.[37–39] Our work then also provides an example of Ostwald's Rule of Stages between crystalline structures.

This work illustrates the possibilities that metastable phases provide for materials discovery and production. Compression of ice Ih outside its stability range and subsequent warming has allowed us to produce a metastable phase C_{-1} that had not previously been observed, as well as allowing us to produce C_0 at significantly lower pressures than had previously been possible. A similar approach might be used for the production of new networks in other network-forming systems (for example silica). An experimental exploration of the metastable phase diagram when combined with computational studies provides insight into the relative stabilities of phases and into the question that is difficult to answer with certainty in studies of phase transitions, that is, which is the stable phase at a given pressure and temperature?

Conflicts of interest

There are no conflicts of interest to declare.

Acknowledgements

The authors would like to thank Chris Goodway, the pressure and furnace and cryogenics teams of the ISIS neutron source for their assistance throughout experiments. We would also like to thank Rachel Husband and Athina Frantzana for their assistance on experiments. We acknowledge support from ISIS the Engineering and Physical Sciences Research Council (EPSRC) through the award of beamtime and associated resources, EPSRC for a departmental training award studentship for MED and a Royal Thai Scholarship for PT.

Notes and references

1 J. S. Loveday and R. J. Nelmes, *Phys. Chem. Chem. Phys.*, 2008, **10**, 937–950.
2 Y. Song, *Phys. Chem. Chem. Phys.*, 2013, **15**, 14524–14547.
3 T. A. Strobel, K. C. Hester, C. A. Koh, A. K. Sum and E. D. Sloan, Jr., *Chem. Phys. Lett.*, 2009, **478**, 97–109.
4 D. M. D'Alessandro, B. Smit and J. R. Long, *Angew. Chem., Int. Ed.*, 2010, **49**, 6058–6082.
5 W. L. Vos, L. W. Finger, R. J. Hemley and H. K. Mao, *Phys. Rev. Lett.*, 1993, **71**, 3150–3153.
6 M. Ozaki, S. Tomura, R. Ohmura and Y. H. Mori, *Int. J. Hydrogen Energy*, 2014, **39**, 3327–3341.
7 R. Kumar, D. D. Klug, C. I. Ratcliffe, C. A. Tulk and J. A. Ripmeester, *Angew. Chem., Int. Ed.*, 2013, **52**, 1531–1534.
8 W. L. Mao, H. K. Mao, A. F. Goncharov, V. V. Struzhkin, Q. Z. Guo, J. Z. Hu, J. F. Shu, R. J. Hemley, M. Somayazulu and Y. S. Zhao, *Science*, 2002, **297**, 2247–2249.

9 K. A. Lokshin, Y. S. Zhao, D. W. He, W. L. Mao, H. K. Mao, R. J. Hemley, M. V. Lobanov and M. Greenblatt, *Phys. Rev. Lett.*, 2004, **93**, 125503.
10 V. S. Efimchenko, M. A. Kuzovnikov, V. K. Fedotov, M. K. Sakharov, S. V. Simonov and M. Tkacz, *J. Alloys Compd.*, 2011, **509**, S860–S863.
11 T. A. Strobel, M. Somayazulu and R. J. Hemley, *J. Phys. Chem. C*, 2011, **115**, 4898–4903.
12 G. S. Smirnov and V. V. Stegailov, *J. Phys. Chem. Lett.*, 2013, **4**, 3560–3564.
13 T. A. Strobel, M. Somayazulu, S. V. Sinogeikin, P. Dera and R. J. Hemley, *J. Am. Chem. Soc.*, 2016, **138**, 13786–13789.
14 D. M. Amos, M.-E. Donnelly, P. Teeratchanan, C. L. Bull, A. Falenty, W. F. Kuhs, A. Hermann and J. S. Loveday, *J. Phys. Lett.*, 2017, **8**, 4295–4299.
15 G.-R. Qian, A. O. Lyakhov, Q. Zhu, A. R. Oganov and X. Dong, *Sci. Rep.*, 2014, **4**, 5606.
16 Deuterated samples were used to avoid the high background scattering caused by the large incoherent neutron cross section of hydrogen.
17 T. L. Malkin, B. J. Murray, C. G. Salzmann, V. Molinero, S. J. Pickering and T. F. Whale, *Phys. Chem. Chem. Phys.*, 2015, **17**, 60–76.
18 M.-E. Donnelly, PhD thesis, The University of Edinburgh, 2016.
19 Y. A. Dyadin, E. Y. Aladko, A. Y. Manakov, F. V. Zhurko, T. V. Mikina, V. Y. Komarov and E. V. Grachev, *J. Struct. Chem.*, 1999, **40**, 790–795.
20 V. E. Antonov, V. S. Efimchenko and M. Tkacz, *J. Phys. Chem. B*, 2009, **113**, 779–785.
21 V. S. Efimchenko, V. E. Antonov, O. I. Barkalov, A. I. Beskrovnyy, V. K. Fedotov and S. N. Klyamkin, *High Press. Res.*, 2006, **26**, 439–443.
22 C. L. Bull, N. P. Funnell, M. G. Tucker, S. Hull, D. J. Francis and W. G. Marshall, *High Press. Res.*, 2016, **7959**, 1–10.
23 O. Arnold, J. C. Bilheux, J. M. Borreguero, A. Buts, S. I. Campbell, L. Chapon, M. Doucet, N. Draper, R. F. Leal, M. A. Gigg, V. E. Lynch, A. Markvardsen, D. J. Mikkelson, R. L. Mikkelson, R. Miller, K. Palmen, P. Parker, G. Passos, T. G. Perring, P. F. Peterson, S. Ren, M. A. Reuter, A. T. Savici, J. W. Taylor, R. J. Taylor, R. Tolchenov, W. Zhou and J. Zikovski, *Nucl. Instrum. Methods Phys. Res., Sect. A*, 2014, **764**, 156.
24 A. C. Larson and R. B. Von Dreele, *Los Alamos National Laboratory Report LAUR*, 1994, pp. 86–748.
25 G. Kresse and J. Furthmüller, *Phys. Rev. B: Condens. Matter Mater. Phys.*, 1996, **54**, 11169–11186.
26 G. Kresse and D. Joubert, *Phys. Rev. B: Condens. Matter Mater. Phys.*, 1999, **59**, 1758–1775.
27 M. Dion, H. Rydberg, E. Schröder, D. C. Langreth and B. I. Lundqvist, *Phys. Rev. Lett.*, 2004, **92**, 246401.
28 G. Román-Pérez and J. M. Soler, *Phys. Rev. Lett.*, 2009, **103**, 096102.
29 J. Klimeš, D. R. Bowler and A. Michaelides, *J. Phys.: Condens. Matter*, 2010, **22**, 022201.
30 J. Klimeš, D. Bowler and A. Michaelides, *Phys. Rev. B: Condens. Matter Mater. Phys.*, 2011, **83**, 195131.
31 A. D. Fortes, I. G. Wood, M. Alfredsson, L. Vočadlo and K. S. Knight, *J. Appl. Crystallogr.*, 2005, **38**, 612–618.
32 C. G. Salzmann, P. G. Radaelli, B. Slater and J. L. Finney, *Phys. Chem. Chem. Phys.*, 2011, **13**, 18468–18480.
33 W. F. Kuhs, C. Sippel, A. Falenty and T. C. Hansen, *Proc. Natl. Acad. Sci. U. S. A.*, 2012, **109**, 21259–21264.
34 P. Teeratchanan, PhD thesis, The University of Edinburgh, 2017.
35 P. Teeratchanan and A. Hermann, *J. Chem. Phys.*, 2015, **143**, 154507.
36 W. Ostwald, *Z. Phys. Chem.*, 1897, **22**, 289–330.
37 S.-Y. Chung, Y.-M. Kim, J.-G. Kim and Y.-J. Kim, *Nat. Phys.*, 2009, **5**, 68–73.
38 D. Cavallo, D. Mileva, G. Portale, L. Zhang, L. Balzano, G. C. Alfonso and R. Androsch, *ACS Macro Lett.*, 2012, **1**, 1051–1055.
39 C. G. Salzmann, E. Mayer and A. Hallbrucker, *Phys. Chem. Chem. Phys.*, 2004, **6**, 5156–5165.